THE JOURNAL OF BIOLOGICAL CHEMISTRY VOL. 289, NO. 44, pp. 30753–30762, October 31, 2014

NirN Protein from *Pseudomonas aeruginosa* is a Novel Electron-bifurcating Dehydrogenase Catalyzing the Last Step of Heme d_1 Biosynthesis*

Received for publication, August 8, 2014, and in revised form, September 3, 2014 Published, JBC Papers in Press, September 9, 2014, DOI 10.1074/jbc.M114.603886

Julia Adamczack[‡], Martin Hoffmann[§], Ulrich Papke[¶], Kristin Haufschildt[‡], Tristan Nicke[‡], Martin Bröring[§], Murat Sezer[‖], Rebecca Weimar[‖], Uwe Kuhlmann[‖], Peter Hildebrandt[‖1], and Gunhild Layer[‡2]

From the [‡]Institute of Microbiology, Technische Universität Braunschweig, Spielmannstr. 7, 38106 Braunschweig, Germany; the [§]Institute of Inorganic and Analytical Chemistry and [¶]Institute of Organic Chemistry, Technische Universität Braunschweig, Hagenring 30, 38106 Braunschweig, Germany; and the [‖]Institute of Chemistry, Technische Universität Berlin, Straße des 17. Juni 135, 10623 Berlin, Germany

Background: Cytochrome cd_1 nitrite reductase contains heme d_1 as an essential cofactor.
Results: *P. aeruginosa* lacking the NirN protein produces the heme d_1 precursor dihydro-heme d_1, which is converted by NirN to heme d_1.
Conclusion: NirN catalyzes the last step of heme d_1 biosynthesis.
Significance: The so far unknown function of NirN is revealed.

Heme d_1 plays an important role in denitrification as the essential cofactor of the cytochrome cd_1 nitrite reductase NirS. At present, the biosynthesis of heme d_1 is only partially understood. The last step of heme d_1 biosynthesis requires a so far unknown enzyme that catalyzes the introduction of a double bond into one of the propionate side chains of the tetrapyrrole yielding the corresponding acrylate side chain. In this study, we show that a *Pseudomonas aeruginosa* PAO1 strain lacking the NirN protein does not produce heme d_1. Instead, the NirS purified from this strain contains the heme d_1 precursor dihydro-heme d_1 lacking the acrylic double bond, as indicated by UV-visible absorption spectroscopy and resonance Raman spectroscopy. Furthermore, the dihydro-heme d_1 was extracted from purified NirS and characterized by UV-visible absorption spectroscopy and finally identified by high-resolution electrospray ionization mass spectrometry. Moreover, we show that purified NirN from *P. aeruginosa* binds the dihydro-heme d_1 and catalyzes the introduction of the acrylic double bond *in vitro*. Strikingly, NirN uses an electron bifurcation mechanism for the two-electron oxidation reaction, during which one electron ends up on its heme *c* cofactor and the second electron reduces the substrate/product from the ferric to the ferrous state. On the basis of our results, we propose novel roles for the proteins NirN and NirF during the biosynthesis of heme d_1.

The process of denitrification, *i.e.* the stepwise reduction of nitrate to molecular nitrogen, represents one important branch of the global biogeochemical nitrogen cycle. Moreover, for denitrifying organisms such as the human pathogen *Pseudomonas aeruginosa*, denitrification serves as a very efficient strategy for energy generation under anaerobic growth conditions (1). In the second step of the denitrification process, nitrite is reduced to nitric oxide. In *P. aeruginosa*, this reaction is catalyzed by the periplasmic cytochrome cd_1 nitrite reductase NirS (2). This enzyme is a homodimer of two 60-kDa subunits, each carrying a heme *c* and a heme d_1 cofactor (3). The non-covalently bound heme d_1 represents the catalytic site of the enzyme where the reduction of nitrite to nitric oxide takes place (4).

Heme d_1 belongs to the tetrapyrrole subfamily of isobacteriochlorins. It carries two unusual carbonyl functions on pyrrole rings A and B and an acrylate side chain on ring D that make heme d_1 unique among the naturally occurring tetrapyrroles (Fig. 1) (5, 6). The biosynthesis of heme d_1 from the common tetrapyrrole precursor uroporphyrinogen III requires six enzymatic steps (7). Most of the involved enzymes are encoded by the *nir* genes, which are located together in the *nir* operon in *P. aeruginosa* (*nirSMCFDLGHJEN*) and also in other denitrifying bacteria (Fig. 1*A*) (8–10). In the first step, the *S*-adenosylmethionine-dependent uroporphyrinogen III methyltransferase NirE catalyzes the methylation of uroporphyrinogen III to precorrin-2 (11, 12). Next, precorrin 2 is converted to siroheme in two enzymatic steps catalyzed by a precorrin-2 dehydrogenase and a sirohydrochlorin ferrochelatase not encoded within the *nir* operon in *P. aeruginosa*. Siroheme is then decarboxylated to 12,18-didecarboxy-siroheme by the action of siroheme decarboxylase, which is composed of the four proteins NirD, NirL, NirG, and NirH (7). The penultimate step of heme d_1 biosynthesis consists of the removal of the two propionate side chains on pyrrole rings A and B, with the concomitant introduction of the carbonyl functions at these positions yielding the heme d_1 precursor dihydro-heme d_1. This transformation is believed to be catalyzed by the radical *S*-adenosylmethionine enzyme NirJ (7). However, this hypothesis still requires experimental proof. Similarly, the enzyme responsible

* This work was supported by Deutsche Forschungsgemeinschaft Grants BR 2010/12-1 (to M. B.) and LA 2412/3-2 (to G. L.).
[1] Supported by the Cluster of Excellence "UniCat" funded by the Deutsche Forschungsgemeinschaft.
[2] To whom correspondence should be addressed: Institute of Microbiology, Technische Universität Braunschweig, Spielmannstr. 7, 38106 Braunschweig, Germany. Tel.: 49-531-391-5803; Fax: 49-531-391-5854; E-mail: g.layer@tu-braunschweig.de.

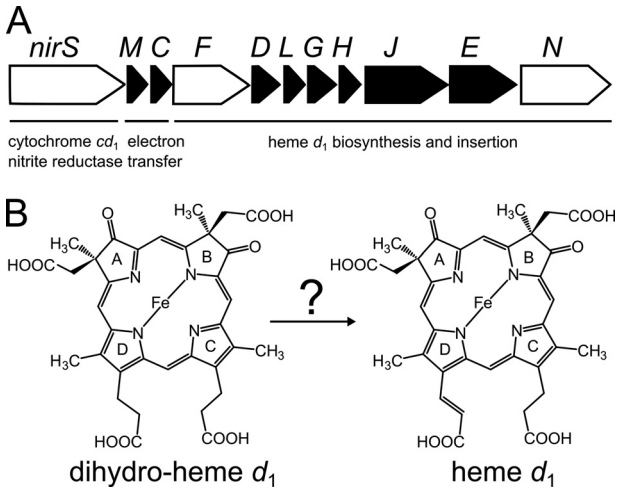

FIGURE 1. **Heme d_1 biosynthesis.** *A*, the *nir* operon from *P. aeruginosa* comprises the genes coding for cytochrome cd_1 nitrite reductase (*nirS*), electron transferring *c*-type cytochromes (*nirM* and *nirC*), and proteins involved in heme d_1 biosynthesis and insertion into NirS (*nirF*, *nirD*, *nirL*, *nirG*, *nirH*, *nirJ*, *nirE*, and *nirN*). The genes encoding proteins used in this study are shown as *white arrows*. *B*, the proposed last step of heme d_1 biosynthesis consists of the introduction of the double bond into the propionate side chain of pyrrole ring D of the precursor dihydro-heme d_1, yielding the acrylate side chain of heme d_1. Until now, the enzyme catalyzing this reaction was not known.

for the last step of heme d_1 biosynthesis has not yet been identified. In this step, the propionate side chain on pyrrole ring D is converted to the corresponding acrylate side chain (Fig. 1*B*). At some stage of its biosynthesis, heme d_1, or a precursor thereof, has to be transported across the cytoplasmic membrane to be incorporated into its target enzyme NirS in the periplasm. Currently it is thought that all heme d_1 biosynthesis steps, except the last one, take place in the cytoplasm and that the final step is catalyzed in the periplasm. This hypothesis is on the basis of the finding that NirF, which has been proposed to catalyze the acrylate group formation, is a periplasmic protein (13), whereas NirE, NirDLGH, and NirJ are located in the cytoplasm.

Depending on the organism, NirF is either a soluble periplasmic protein or attached to the outer face of the cytoplasmic membrane, most likely by a lipid anchor (14, 15). In addition to its periplasmic location, purified recombinant NirF from *Paracoccus pantotrophus* has been shown to bind heme d_1 *in vitro* (13). Moreover, early mutational studies with different denitrifying bacteria have shown that the deletion of the *nirF* gene results in bacterial strains unable to synthesize heme d_1 (8–10, 13). On the basis of all of these findings, NirF has been proposed to catalyze the formation of the acrylic double bond of heme d_1. However, so far there is no direct experimental evidence clearly attributing this enzymatic function to NirF.

Interestingly, another *nir* gene (*nirN*) is present in all denitrifying bacteria. The encoded NirN protein shares about 24% amino acid sequence identity with NirS. Moreover, NirN has been shown to be located in the periplasm and to contain a heme *c* cofactor (16). The monomeric NirN was able to bind heme d_1 *in vitro* and transferred the cofactor to NirS when the two proteins were mixed (12). The deletion of the *nirN* gene in different denitrifiers led to a mild growth phenotype, and cell-free extracts prepared from the corresponding Δ*nirN* strains exhibited reduced NirS activity compared with the WT strains (9, 12, 16). From these observations it was deduced that NirN is not required for heme d_1 biosynthesis but, rather, might be involved in the insertion of the cofactor into NirS. In line with this proposal it has been shown that NirN from *P. aeruginosa* interacts with both NirS and NirF *in vivo*. However, in that study it was also observed by UV-visible absorption spectroscopy of periplasmic protein fractions that the cofactor content of NirS in the *P. aeruginosa* Δ*nirN* strain was different from that in the *P. aeruginosa* WT strain (15). Later, the same observation was reported for a Δ*nirN* strain of *Magnetospirillum gryphiswaldense* (17).

The apparently altered cofactor content of NirS in these Δ*nirN* strains can be rationalized by two different hypothetical scenarios: (i) NirN is involved in heme d_1 insertion into NirS, and the absence of NirN leads to an improper incorporation of the cofactor causing the observed spectral differences, or (ii) NirN is involved in the last step of heme d_1 biosynthesis (together with NirF?), and the absence of NirN leads to the accumulation of dihydro-heme d_1, which is nevertheless inserted into NirS, leading to a different form of holo NirS with different spectral properties and reduced enzyme activity. Therefore, the aim of this study was to investigate and clarify the still enigmatic function of NirN during either heme d_1 biosynthesis or insertion into NirS.

EXPERIMENTAL PROCEDURES

Chemicals—Chemicals and reagents were obtained from Sigma-Aldrich (Taufkirchen, Germany), Merck (Darmstadt, Germany), or Thermo Fisher Scientific Inc. (Schwerte, Germany). Restriction endonucleases were purchased from New England Biolabs (Frankfurt am Main, Germany). QIAquick PCR purification and gel extraction kits were purchased from Qiagen GmbH (Hilden, Germany). Q-Sepharose Fast Flow and SP-Sepharose Fast Flow were obtained from GE Healthcare. Strep-Tactin-HC resin, Desthiobiotin, and Avidin were purchased from IBA GmbH (Göttingen, Germany). All oligonucleotide primers were obtained from Metabion International AG (Martinsried, Germany).

Plasmids and Strains—The *Escherichia coli* strain BL21(DE3) was used as a host for protein production of recombinant semi-apo NirS ($NirS_{s.a.}$), NirN, and NirF. For the production of $NirS_{s.a.}$ and NirN, *E. coli* BL21(DE3) was transformed with the plasmid pEC86 (provided by Dr. Linda Thöny-Meyer (18)) and either pET-22b(+)*nirS* (15) or pET-22b(+)StrepII*nirN*. For the production of recombinant NirF from *Dinoroseobacter shibae*, *E. coli* BL21(DE3) was transformed with pET-22b(+)$nirF_{(D.s.)}$PCSStrepII. The *P. aeruginosa* PAO1 WT strain was used for protein production of native holo NirS ($NirS_{WT}$). For protein production of native NirS containing dihydro-heme d_1 ($NirS_{\Delta N}$), the *P. aeruginosa* PAO1 strain RM361 (*nirN*::*tet*) was used (provided by Dr. Hiroyuki Arai (9)).

Construction of Vectors—For the construction of a NirN expression vector, the *nirN* gene from *P. aeruginosa* PAO1 was PCR-amplified using the primers strepII*nirN*_fw (TAT A<u>CC ATG G</u>GC TGG AGC CAC CCG CAG TTC GAA AAA GCT AGC GGC GAA GCG CCG GGG GAA G) and *nirN*_rev (CG <u>*GGA TCC*</u> TCA GTG CGA GGT TC), which contained NcoI and BamHI restriction sites (underlined), respectively. The di-

gested *nirN* insert was ligated into the correspondingly digested vector pET-22b(+) to generate pET-22b(+)StrepII*nirN*. For the construction of an expression vector for NirF from *D. shibae*, the plasmid pMK-RQ*rbspelBnirF*$_{(D.s.)}$PCS*his*$_6$ was purchased from Invitrogen. Through restriction of the plasmid with NdeI and HindIII, the insert pelB*nirF*$_{(D.s.)}$PCShis$_6$ was obtained and ligated into the correspondingly digested plasmid pET-22b(+). A Strep tag coding insert was obtained by annealing the primers CTA GTA GCG CTT GGA GCC ACC CGC AGT TCG AAA AAG and GAT CCT TTT TCG AAC TGC GGG TGG CTC CAA GCG CTA. The His tag coding sequence was removed from pET-22b(+)pelB*nirF*$_{(D.s.)}$PCShis$_6$ using SpeI and BamHI restriction sites, and the Strep tag coding insert was ligated into pET-22b(+)pel B*nirF*$_{(D.s.)}$PCS to generate pET-22b(+)*nirF*$_{(D.s.)}$PCSStrepII.

Growth Conditions—E. coli BL21(DE3) carrying the plasmids pEC86 and pET-22b(+)*nirS* or pET-22b(+)StrepII*nirN* for the production of NirS$_{s.a.}$ (containing the covalently bound heme *c* but no heme d_1) and heme *c* containing NirN, respectively, were grown according to Studier (19) in self-inducing ZYM5052 medium containing 100 μg/ml ampicillin and 34 μg/ml chloramphenicol for 4 h at 37 °C and, subsequently, for 26 h at 25 °C. *E. coli* BL21(DE3) carrying the plasmid pET-22b(+)-*nirF*$_{(D.s.)}$PCSStrepII was grown in terrific broth (20) containing 100 μg/ml ampicillin to an optical density of 0.8 at 37 °C and, after induction with 100 μM isopropyl 1-thio-β-D-galactopyranoside, for 26 h at 17 °C. For the production of native NirS containing heme *c* and heme d_1 or dihydro-heme d_1, *P. aeruginosa* PAO1 WT or RM361, respectively, were grown under anaerobic conditions for 24 h at 37 °C in autoinducer bioassay minimal medium (according to Heydorn *et al.* (21)) supplied with 75 mM $NaNO_3$ and 7.5 μM 5-aminolevulinic acid.

Purification of Proteins—The purifications of recombinant *P. aeruginosa* NirS$_{s.a.}$, native holo NirS$_{WT}$, and NirS$_{\Delta N}$ were performed according to Parr *et al.* (22). Recombinant NirN and NirF were purified using Strep-Tactin-HC resin according to the instructions of the manufacturer (IBA GmbH) and with 50 mM Tris-HCl (pH 7.5), 150 mM NaCl as the buffer.

Determination of Protein Concentration—Bradford reagent (Sigma-Aldrich) was used to determine protein concentrations. The reagent was used according to the instructions of the manufacturer using BSA as a standard.

Extraction of Nitrite Reductase Cofactors—Heme d_1 and dihydro-heme d_1 were extracted from purified NirS$_{WT}$ and NirS$_{\Delta N,}$ respectively. Proteins at a concentration of 90 μM in buffer (50 mM Tris-HCl (pH 7.5), 150 mM NaCl) were precipitated with 6 mM HCl. Two volumes of ethyl acetate (HPLC grade) were added, and the samples were mixed for 1 min and then centrifuged for 2 min at 13000 $\times$ *g*. The organic cofactor-containing phase was removed and dried *in vacuo*. For HR-ESI-MS analysis,[3] proteins were transferred to double distilled water prior to the extraction of the cofactors, and the dried cofactors were dissolved in methanol.

UV-visible Absorption Spectroscopy—UV-visible absorption spectra of purified proteins and extracted cofactors were recorded using a V-650 spectrophotometer (Jasco, Gross-Umstadt, Germany). The reduced forms of proteins and isolated cofactors were obtained by addition of a few grains of sodium dithionite.

Resonance Raman Spectroscopy—RR spectra with a spectral resolution of 2 cm^{-1} were recorded using a confocal Raman spectrometer (Lab Ram HR-800, Jobin Yvon) equipped with a liquid nitrogen-cooled charge-coupled device camera. The 442-nm excitation line of a He-Cd laser (Soliton) was focused onto the sample (2 μm in diameter, 1 milliwatt at the sample). Using a Linkam Cryostage THMS600 cryostat, the temperature of the sample was set to 80 K throughout the measurement. Raman shifts were calibrated to an accuracy of 0.5 cm^{-1} using toluene as an external standard. All spectra were corrected by polynomial background subtraction.

Heme d_1 and Dihydro-Heme d_1 Binding to NirN and NirF—For binding of heme d_1 and dihydro-heme d_1 to NirN and NirF, the *in vacuo* dried cofactors were directly dissolved in 150 μl of buffer (50 mM Tris-HCl (pH 7.5), 150 mM NaCl) containing either NirN at a concentration of 20 μM or NirF at a concentration of 38 μM. Directly after mixing, UV-visible absorption spectra of the mixtures were recorded on a V-650 spectrophotometer (Jasco).

NirN Activity Assay, Transfer of Cofactors to NirS$_{s.a.}$, and Reconstitution of NirS$_{s.a.}$—The *in vitro* NirN activity assay was performed under aerobic or anaerobic conditions in an anaerobic chamber (Coy Laboratories, Grass Lake, MI). For the aerobic assay, dried dihydro-heme d_1 was dissolved in buffer (50 mM Tris-HCl (pH 7.5), 150 mM NaCl) and transferred to a quartz cuvette (Hellma Analytics, Müllheim, Germany). NirN was subsequently added at a final concentration of 20 μM to give a final volume of 150 μl. For the anaerobic assay, the dried dihydro-heme d_1 was dissolved in degassed buffer in the anaerobic chamber, followed by the addition of 20 μM NirN under anaerobic conditions. The NirN-catalyzed reaction was monitored using a V-650 spectrophotometer (Jasco). For the reconstitution of NirS$_{s.a.}$ with heme d_1 or dihydro-heme d_1 and the transfer of the NirN reaction product to NirS$_{s.a.}$, the enzyme was added to the NirN assay or the cofactor solution at a final concentration of 20 μM. For the oxidation of heme d_1, sodium persulfate was added.

HR-ESI-MS (Accurate Mass Measurements) of Nitrite Reductase Cofactors—The sample solutions obtained after cofactor extraction were used for accurate mass measurements on an LTQ-Orbitrap Velos (ThermoFisher Scientific, Bremen, Germany). Electrospray measurements in positive mode were performed in direct infusion mode using a custom-made microspray device mounted on a Proxeon nanospray ion source. The microspray device allows sample infusion without sheath gas through a stainless steel capillary (90-μm inner diameter) at a flow rate of ~1 μl/min. The spray voltage was set between 2.0 and 2.3 kV. The resolution of the Orbitrap mass analyzer was set to 100,000 full width at half-maximum (FWHM) at *m*/*z* 400. Accurate mass measurements were performed using the lock mass option of the instrument control software using the cation of tetradecyl-trimethylammonium bromide (256.29988 u) as an internal mass reference, which was added to the sample solution in appropriate amounts.

[3] The abbreviations used are: HR-ESI-MS, high-resolution electrospray ionization MS; RR, resonance Raman.

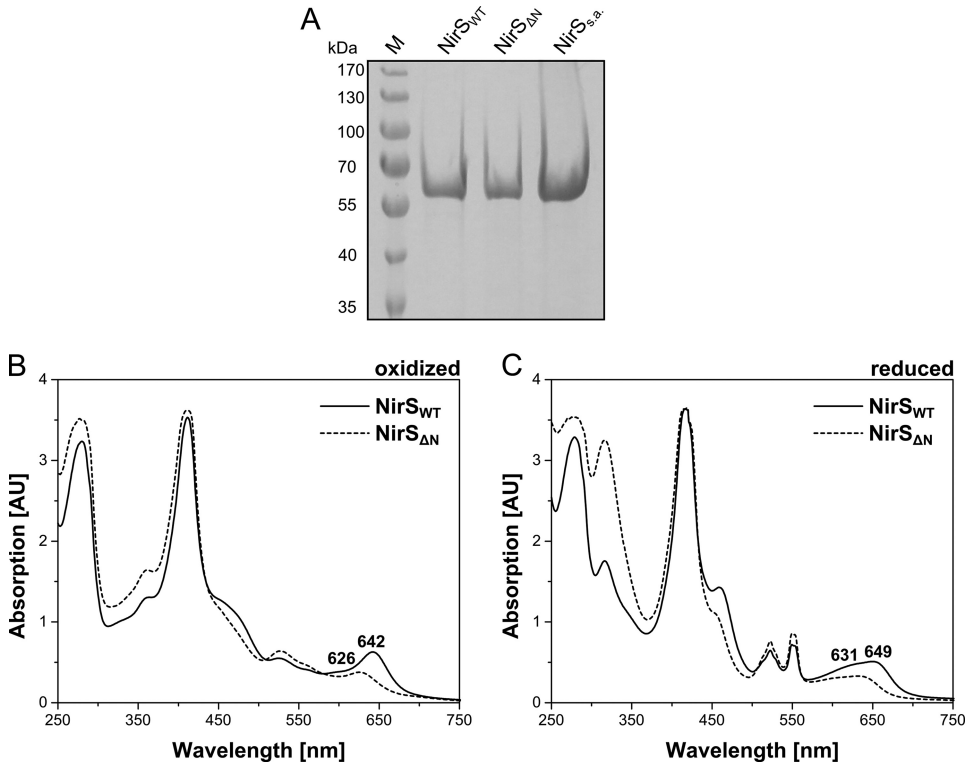

FIGURE 2. **Purification and characterization of NirS$_{WT}$ and NirS$_{\Delta N}$.** *A*, SDS-PAGE analysis of purified native NirS$_{WT}$ and NirS$_{\Delta N}$ and recombinant NirS$_{s.a.}$ from *P. aeruginosa*. *Lane M* shows marker proteins with M_r values indicated. *B* and *C*, UV-visible absorption spectra of purified native NirS$_{WT}$ and NirS$_{\Delta N}$ in the oxidized (as-isolated) (*B*) and dithionite-reduced (*C*) forms. Characteristic absorption bands are labeled. *AU*, absorption units.

RESULTS AND DISCUSSION

*Purification of Native NirS from the P. aeruginosa PAO1 Δ*nirN* Strain RM361*—To obtain more insights into the role of NirN, the first aim of this study was to purify NirS from the *P. aeruginosa* PAO1 Δ*nirN* strain RM361 and to characterize the cofactor content of this apparently different form of holo NirS. Previous attempts to purify native NirS from the *P. aeruginosa* PAO1 strain RM361 only resulted in the isolation of semi-apo NirS (NirS$_{s.a.}$) completely lacking heme d_1 (15). Therefore, the purification protocol was changed slightly, including the reduction of the column volume of the anion exchange chromatography column. Using the new purification procedure, NirS was purified to apparent homogeneity (Fig. 2*A*). The enzyme purified from strain RM361 (NirS$_{\Delta N}$) exhibited a less intense green color in contrast to the green color of NirS isolated from the WT strain (NirS$_{WT}$) and the red colored semi-apo form of NirS lacking heme d_1. This observation clearly supports the idea that a different form of holo NirS was produced in the *P. aeruginosa* Δ*nirN* strain.

UV-visible Absorption Spectroscopy of Purified NirS$_{\Delta N}$ and NirS$_{WT}$—To characterize the cofactor content of NirS$_{\Delta N}$, UV-visible absorption spectra of the purified enzyme were recorded of the oxidized (as isolated) and dithionite-reduced forms and compared with the corresponding spectra of purified NirS$_{WT}$ (Fig. 2, *B* and *C*). The absorption spectra of NirS$_{\Delta N}$ are clearly different from those of NirS$_{WT}$ in both the oxidized and reduced forms. In fact, the spectra of the two enzymes differ, particularly in the region of the characteristic heme d_1 absorption bands. Although the spectrum of oxidized NirS$_{WT}$ exhibits a typical heme d_1 peak at 642 nm, the spectrum of NirS$_{\Delta N}$ shows a peak at 626 nm. In the reduced form, the heme d_1 absorption band of NirS$_{WT}$ is shifted to 649 nm, whereas, for NirS$_{\Delta N}$, a peak shift to 631 nm is observed. These spectral differences between the purified NirS$_{\Delta N}$ and NirS$_{WT}$ confirmed the presence of two different forms of holo NirS depending on whether the enzyme was isolated from *P. aeruginosa* PAO1 strain RM361 or from the WT strain. There were two possible explanations for the observed spectral differences. Either heme d_1 was not properly inserted into NirS$_{\Delta N}$ and the observed differences were due to a different ligation of the cofactor, or it was not heme d_1 but the precursor dihydro-heme d_1 that was present in NirS$_{\Delta N}$. On the basis of the observed UV-visible absorption spectra of NirS$_{\Delta N}$, we favored the second hypothesis. The conjugated system of dihydro-heme d_1 lacks one double bond compared with heme d_1. For this reason, the absorption maxima of dihydro-heme d_1 can be expected to be located at shorter wavelengths than those of heme d_1 (hypsochromic shift). Indeed, such a shift was observed for the absorption maximum of NirS$_{\Delta N}$ (626 nm, oxidized) compared with the heme d_1-containing NirS$_{WT}$ (642 nm, oxidized).

Resonance Raman Spectroscopy of NirS$_{\Delta N}$, NirS$_{WT}$ and NirS$_{s.a.}$—To further characterize the unusual cofactor content of NirS$_{\Delta N}$ and to obtain more insights into the question of whether dihydro-heme d_1 is indeed bound in NirS$_{\Delta N}$, resonance Raman (RR) spectroscopy was performed. RR spectra of purified NirS$_{WT}$, NirS$_{\Delta N}$, and semi-apo NirS were measured at low temperature to reduce the strong background scattering and to increase the signal-to-noise ratio. Although, upon 413-nm excitation, the heme *c* bands were selectively enhanced (data not shown), 442-nm excitation led to a substantial

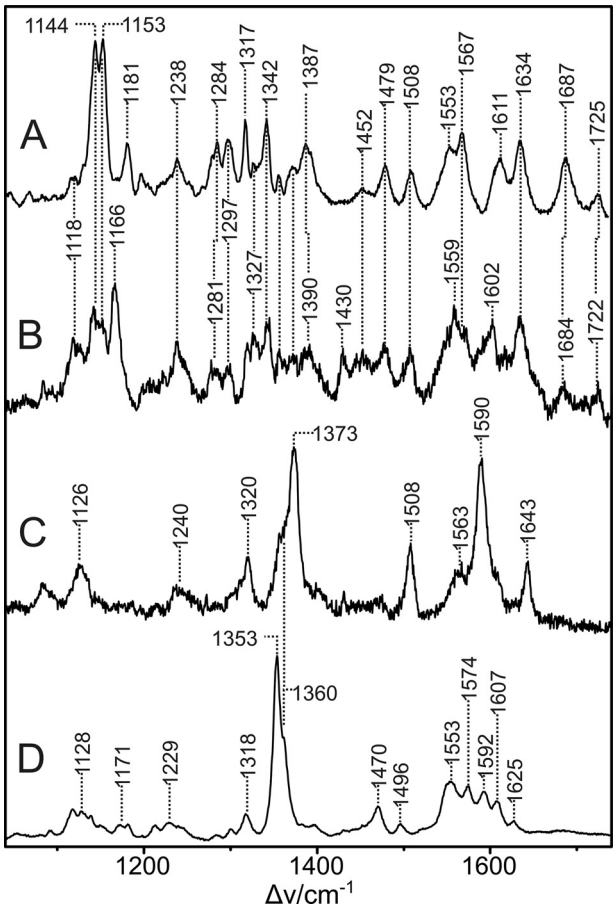

FIGURE 3. **RR spectra of $NirS_{WT}$, $NirS_{\Delta N}$, and semi-apo NirS measured with 442-nm excitation at 80 K.** *A*, oxidized heme d_1 of $NirS_{WT}$. *B*, oxidized dihydro-heme d_1 of $NirS_{\Delta N}$. *C*, oxidized heme *c* of semi-apo NirS. *D*, reduced heme *c* of semi-apo NirS. The spectra in *A* and *B* were obtained by subtracting the heme *c* contributions (spectra *C* and *D*) from the spectra of the (as-isolated) enzymes $NirS_{WT}$ and $NirS_{\Delta N}$, respectively. The spectra of the oxidized heme *c* (*C*) and reduced heme *c* (*D*) were generated by mutual spectra subtraction of the as-isolated (mainly oxidized) and dithionite-reduced semi-apo NirS because the spectrum of the pure oxidized semi-apo NirS cannot be measured directly because of photoreduction at low temperatures. Note that the ferrous heme *c* in semi-apo NirS undergoes an unprecedented reversible temperature-dependent transition from the low-spin to the high-spin configuration. The latter prevails at 80 K, as indicated by the characteristic marker bands at 1353, 1470, and 1607 cm^{-1} (24, 32).

increase of the spectral mass of heme d_1 and the putative dihydro-heme d_1 in $NirS_{WT}$ and $NirS_{\Delta N}$, respectively. Remaining contributions of heme *c* could readily be removed by subtracting the spectra of $NirS_{s.a.}$ from those of $NirS_{WT}$ and $NirS_{\Delta N}$, using the characteristic bands of heme *c* as a reference (Fig. 3, *C* and *D*). Therefore, pure spectra of heme d_1 and the putative precursor were obtained in the oxidized (as-isolated) state (Fig. 3, *A* and B). The spectrum of ferric heme d_1 (Fig. 3*A*) differs substantially from that of heme *c*, which, because of its higher symmetry (D_{4h}), is dominated by the totally symmetric A_{1g} modes (Fig. 3*C*) (23). In contrast, the low symmetry of heme d_1 leads to numerous RR-active modes that are not related to the heme *c* bands. As a consequence, well established empirical relationships for iron porphyrins between band frequencies above 1300 cm^{-1} and the oxidation, spin, and coordination state of iron (24) cannot be extended to heme d_1 and, therefore, most of its bands must remain unassigned. Remarkable exceptions are the bands at 1687 and 1725 cm^{-1}, which originate from the C=O stretching modes of the keto groups and the carboxyl function of the acrylic side chain, respectively. Note that differences between the spectrum in Fig. 3*A* and a spectrum of oxidized cd_1 published previously (25) are likely to be due to different excitation lines and temperatures.

As already expected from the weaker absorbance at 442 nm for $NirS_{\Delta N}$ compared with $NirS_{WT}$ (Fig. 2), the RR spectrum of the putative heme d_1 precursor suffers from a substantially weaker resonance enhancement compared with heme d_1 (Fig. 3*B*). Despite the relatively poor signal-to-noise ratio, the comparison of both spectra demonstrates that most of the bands of heme d_1 also have counterparts within $\pm$ 3 cm^{-1} in the spectrum of the potential heme d_1 precursor, albeit with quite different relative intensities. Therefore, we conclude that the ground state structure of heme d_1 and its precursor are similar but not identical. This conclusion is consistent with the assignment of the heme d_1 precursor to a dihydro-heme d_1. Moreover, among the few bands of $NirS_{WT}$ for which conjugate bands in $NirS_{\Delta N}$ are not immediately evident, the bands at 1611 and 1181 cm^{-1} may be attributed to modes involving the C=C and C-(C=C) stretching coordinates, taking into account previous assignments of modes involving the vinyl substituents in protoporphyin IX (26–29). Furthermore, assuming a dihydro-heme d_1 in $NirS_{\Delta N}$, the different intensity pattern compared with the spectrum of heme d_1 can readily be understood because the extension of the delocalized π-electron system affects both the absolute and relative RR intensities.

$NirS_{\Delta N}$ Contains Dihydro-Heme d_1—The results of the experiments described so far strongly suggest that the heme d_1 precursor dihydro-heme d_1 might indeed be bound in $NirS_{\Delta N}$. To finally clarify this question, the non-covalently bound heme d_1 (or possibly dihydro-heme d_1) was extracted from the purified $NirS_{WT}$ and $NirS_{\Delta N}$ as described under "Experimental Procedures." Then, UV-visible absorption spectra of the oxidized and dithionite-reduced forms were recorded (Fig. 4, *A* and *B*). The absorption spectrum of the heme d_1 cofactor extracted from $NirS_{WT}$ exhibits characteristic peaks at 408 and 683 nm and a shoulder at about 476 nm in the oxidized state, as reported previously (30, 31). In contrast, the spectrum of the oxidized form of the cofactor extracted from $NirS_{\Delta N}$ shows absorption maxima at 397 and 671 nm and also a shoulder at about 476 nm. After dithionite reduction, the absorption bands of the heme d_1 extracted from $NirS_{WT}$ are shifted to 457 and 627 nm, whereas those of the cofactor extracted from $NirS_{\Delta N}$ are shifted to 447 and 611 nm. Again, these observations strongly suggest that the cofactor isolated from $NirS_{\Delta N}$ was indeed different from the heme d_1 extracted from $NirS_{WT}$. As described above, we suspected that the heme d_1 precursor dihydro-heme d_1 lacking the acrylic double bond might be present in $NirS_{\Delta N}$. The UV-visible absorption spectra of the isolated cofactor are in line with this proposal because the characteristic heme d_1 absorption band at 683 nm in the oxidized state is shifted to a shorter wavelength by about 10 nm in the case of the cofactor from $NirS_{\Delta N}$, and the corresponding band of heme d_1 in the reduced state at 627 nm is shifted by about 15 nm in this case. Such a hypsochromic shift would be expected for dihydro-heme d_1 because of the lacking double bond (6).

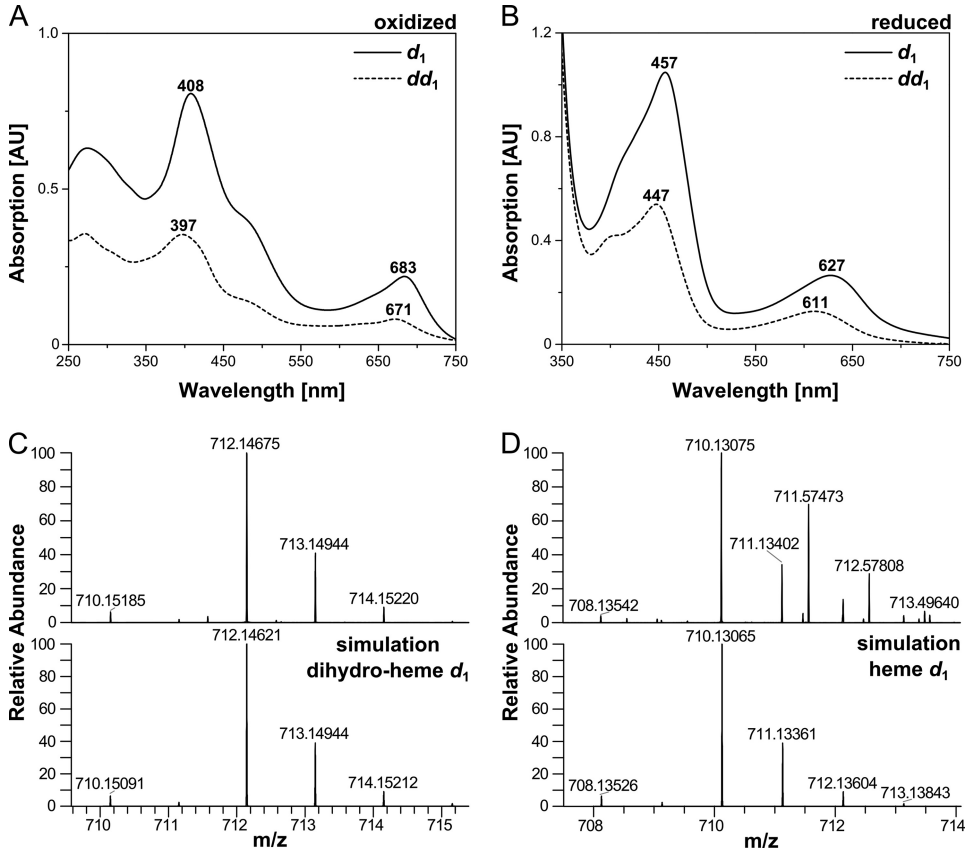

FIGURE 4. **Characterization of cofactors extracted from $NirS_{WT}$ and $NirS_{\Delta N}$.** *A* and *B*, UV-visible absorption spectra of heme d_1 extracted from purified $NirS_{WT}$ (d_1) and of dihydro-heme d_1 extracted from purified $NirS_{\Delta N}$ (dd_1) in the oxidized (as-isolated) (*A*) and dithionite-reduced (*B*) forms. Characteristic absorption bands are labeled. *C* and *D*, HR-ESI-MS analysis of the dihydro-heme d_1 extracted from $NirS_{\Delta N}$ (*C*) and of heme d_1 extracted from $NirS_{WT}$ (*D*). The *top panels* show the experimental mass and isotopic pattern of the $[M+H]^+$ ions, and the *bottom panels* show the calculated mass spectra of dihydro-heme d_1 (*C*) and heme d_1 (*D*), respectively. Note that the measured masses 711.57473, 712.57808, and 713.49640 in *D* originate from an uncharacterized impurity present in the heme d_1 sample. *AU*, absorption units.

Finally, we determined the exact mass of the cofactor extracted from $NirS_{\Delta N}$ by HR-ESI-MS. This method revealed a mass of 712.14675 for the $[M+H]^+$ ion, which is indeed in accordance with the calculated mass (712.14621), isotopic pattern and chemical formula of dihydro-heme d_1 (Fig. 4*C*). For comparison, the mass of the heme d_1 extracted from $NirS_{WT}$ was also determined by HR-ESI-MS. The measured value of 710.13075 for the $[M+H]^+$ ion is in excellent agreement with the theoretical mass (710.13065), isotopic pattern and chemical formula of heme d_1 as expected (Fig. 4*D*). Moreover, the mass difference between the two cofactors isolated from either $NirS_{\Delta N}$ or $NirS_{WT}$ corresponds to the two hydrogen atoms that are present in dihydro-heme d_1 ($NirS_{\Delta N}$) but absent in heme d_1 ($NirS_{WT}$) because of the dehydrogenation of the propionate side chain of pyrrole ring D.

On the basis of all of the results described so far, we conclude that, in the absence of NirN in the bacterial cell, the formation of the acrylic double bond of heme d_1 does not take place and that dihydro-heme d_1 is inserted into $NirS_{\Delta N}$. This novel finding led to the question whether NirN itself catalyzes the dehydrogenation reaction, which would be completely unexpected, or whether NirF catalyzes the double bond formation, as proposed previously, but with the help of NirN. These two possibilities were tested *in vitro*, and the results are described in the following section.

Purified, Recombinant NirN from P. aeruginosa Catalyzes the Conversion of Dihydro-heme d_1 to Heme d_1 in Vitro—To test whether NirN is able to catalyze the dehydrogenation of the propionate side chain of pyrrole ring D, yielding the acrylate side chain of heme d_1, the extracted dihydro-heme d_1 was mixed with purified NirN, and UV-visible absorption spectra were recorded at different time points after mixing. As shown in Fig. 5*A*, the absorption band of the free dihydro-heme d_1 at 671 nm disappeared upon addition of NirN, and a new absorption band at 609 nm was visible immediately after mixing. This new absorption feature most likely represents the binding of dihydro-heme d_1 to NirN. However, after 15 s of incubation, the spectrum had changed, and the absorption band at 609 nm had developed into a broad band at about 635 nm that did not change further during prolonged incubation. On the basis of this observation, we speculated that NirN might have catalyzed the formation of the acrylic double bond after the initial binding of the dihydro-heme d_1 to the enzyme. Therefore, we compared the final absorption spectrum of the NirN/dihydro-heme d_1 reaction mixture with the absorption spectra of a NirN/heme d_1 mixture in the oxidized and reduced states (Fig. 5*B*). Strikingly, the final spectrum of the NirN/dihydro-heme d_1 reaction mixture was identical to the spectrum of the NirN/heme d_1 mixture in the reduced state, both showing an absorption band at 635 nm. Furthermore, we then oxidized the NirN

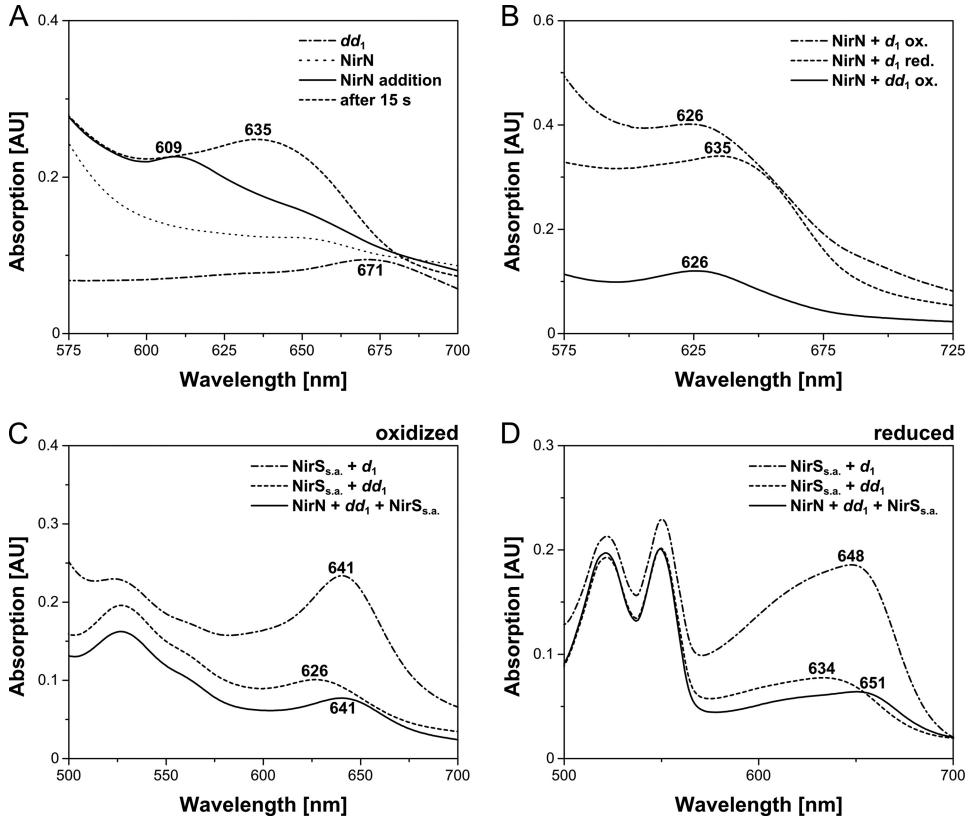

FIGURE 5. **Binding of dihydro-heme d_1 to purified NirN and transfer to semi-apo NirS.** *A*, UV-visible absorption spectra of the free dihydro-heme d_1 (dd_1), of purified NirN, and of the NirN/dihydro-heme d_1 mixture measured immediately after mixing the two components (*NirN addition*) and measured after 15 s of incubation. Characteristic absorption bands are labeled. *B*, UV-visible absorption spectra of NirN/heme d_1 (d_1) mixtures in the oxidized and reduced forms and of the NirN/dihydro-heme d_1 mixture after incubation for several minutes and subsequent oxidation with sodium persulfate. The spectra in *A* indicate that dihydro-heme d_1 first bound to NirN, resulting in a new absorption band at 609 nm, and was then transformed into a new species exhibiting an absorption band at 635 nm. Upon oxidation with sodium persulfate, this species showed an absorption band at 626 nm (*B*). The comparison of these spectra with those of the NirN/heme d_1 mixture (oxidized (*ox.*) and reduced (*red.*)) suggested that NirN catalyzed the transformation of dihydro-heme d_1 to heme d_1. *C* and *D*, UV-visible absorption spectra of the NirN/dihydro-heme d_1 mixture after several minutes of incubation and subsequent addition of $NirS_{s.a.}$ (*NirN* + dd_1 + $NirS_{s.a.}$) and of $NirS_{s.a.}$/heme d_1 and $NirS_{s.a.}$/dihydro-heme d_1 mixtures in the oxidized (*C*) and reduced (*D*) forms. The comparison of the obtained spectra suggested that the cofactor that was transferred from NirN to $NirS_{s.a.}$ after incubation of NirN with dihydro-heme d_1 was indeed the newly formed heme d_1. *AU*, absorption units.

reaction mixture initially containing dihydro-heme d_1 by the addition of sodium persulfate, which resulted in a shift of the 635 nm absorption band to 626 nm. The obtained absorption spectrum was now identical to the spectrum of the NirN/heme d_1 mixture in the oxidized state (Fig. 5*B*). These results suggest that NirN is indeed able to catalyze the conversion of dihydro-heme d_1 to heme d_1.

To further substantiate this finding, we added $NirS_{s.a.}$ to the NirN/dihydro-heme d_1 reaction mixture after the potential conversion of the precursor to heme d_1 was completed. Because it has been reported previously that heme d_1-loaded NirN is able to transfer the cofactor to $NirS_{s.a.}$ (12), we assumed that this transfer should also take place in our reaction mixture. After several minutes of incubation with $NirS_{s.a.}$, UV-visible absorption spectra were recorded. As shown in Fig. 5*C*, the absorption band at 626 nm potentially representing heme d_1-loaded NirN (oxidized) was shifted to 641 nm upon addition of $NirS_{s.a.}$. Indeed, the newly obtained spectrum was identical to the spectrum of heme d_1-containing NirS. Moreover, the same was true after the reduction of the cofactor with sodium dithionite (Fig. 5*D*). These observations clearly supported the idea that NirN catalyzed the conversion of dihydro-heme d_1 to heme d_1. The subsequent transfer of the formed heme d_1 to $NirS_{s.a.}$ yielding holo-NirS took place as described previously (12).

Finally, to unambiguously demonstrate that heme d_1 was formed out of dihydro-heme d_1 by the action of NirN, we extracted the cofactor from the NirN/dihydro-heme d_1 reaction mixture after the reaction was completed and analyzed the formed reaction product by UV-visible absorption spectroscopy and HR-ESI-MS (Fig. 6). The extracted reaction product exhibited an absorption band at 683 nm identical to heme d_1. Moreover, a mass of 710.13043 was determined for the reaction product ($[M+H]^+$), which is in agreement with the theoretical mass (710.13065) of heme d_1. Therefore, we concluded that NirN indeed catalyzed the formation of the acrylic double bond, therefore converting dihydro-heme d_1 to heme d_1.

Purified, Recombinant NirF from D. shibae Binds Dihydro-Heme d_1 without Conversion to Heme d_1—The finding that NirN catalyzes the conversion of dihydro-heme d_1 to heme d_1 was completely unexpected because NirF was originally proposed to be responsible for this reaction. This proposal was made on the basis of the observation that the periplasmic NirF from *P. pantotrophus* was able to bind heme d_1 *in vitro*, and the obtained NirF-heme d_1 complex was interpreted to represent an enzyme-product com-

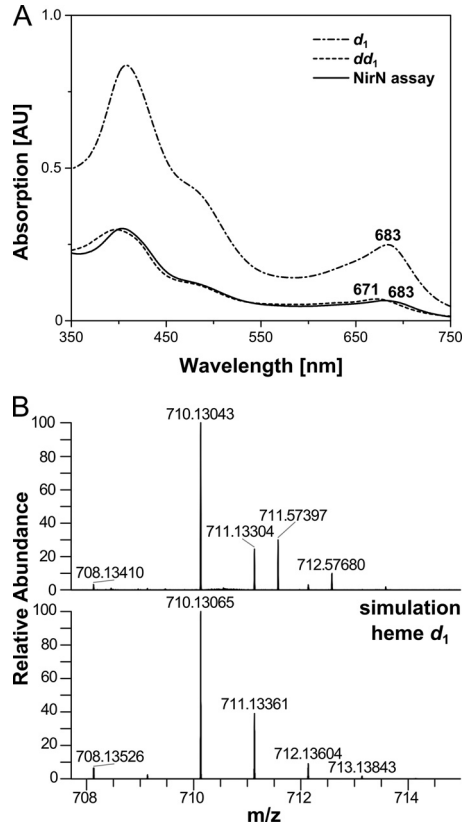

FIGURE 6. **Characterization of the cofactor extracted from the NirN/dihydro-heme d_1 mixture.** *A*, UV-visible absorption spectra of the cofactor extracted from the NirN/dihydro-heme d_1 reaction mixture after several minutes of incubation (*NirN assay*) and spectra of extracted heme d_1 (d_1) and dihydro-heme d_1 (dd_1) for comparison. Characteristic absorption bands are labeled. *B*, HR-ESI-MS analysis of the cofactor extracted from the NirN/dihydro-heme d_1 reaction mixture. The *top panel* shows the experimental mass and isotopic pattern of the $[M+H]^+$ ion, and the *bottom panel* shows the calculated mass spectrum of heme d_1. Note that the measured masses 711.57397 and 712.57680 originate from an uncharacterized impurity present in the sample. *AU*, absorption units.

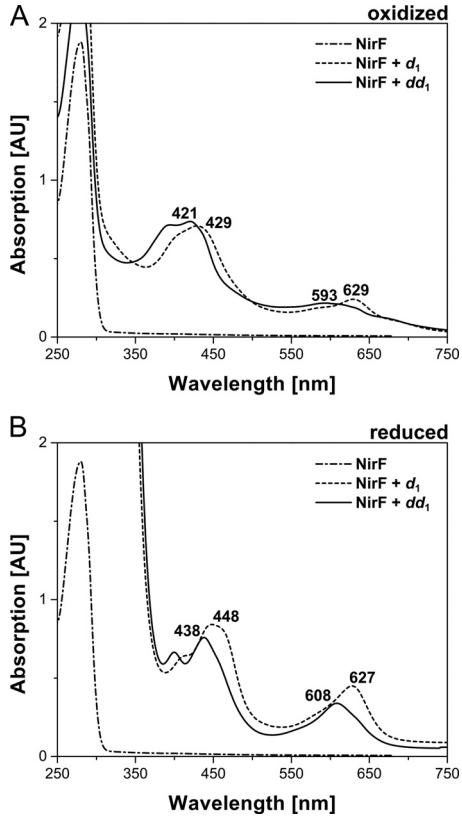

FIGURE 7. **Binding of heme d_1 and dihydro-heme d_1 to purified NirF.** *A* and *B*, UV-visible absorption spectra of purified NirF, NirF incubated with heme d_1 (d_1), and NirF incubated with dihydro-heme d_1 (dd_1). Spectra were measured in the oxidized (*A*) and dithionite-reduced (*B*) forms. Characteristic absorption bands are labeled. *AU*, absorption units.

plex (13). Therefore, we incubated purified, recombinant NirF from *D. shibae* with dihydro-heme d_1 and heme d_1, and the binding of the cofactors to the protein was followed by UV-visible absorption spectroscopy (Fig. 7). The spectrum of the NirF/heme d_1 mixture exhibits characteristic absorption bands at 429 and 629 nm in the oxidized state and at 448 and 627 nm in the reduced form, which is in agreement with the absorption features of heme d_1-containing NirF from *P. pantotrophus* reported previously (13). The spectrum of the NirF/dihydro-heme d_1 mixture displays absorption bands at 421 and 593 nm in the oxidized form and at 438 and 608 nm in the reduced form, showing that NirF is also able to bind the dihydro-heme d_1 precursor because the observed absorption features of the NirF/dihydro-heme d_1 mixture clearly differ from those of the free dihydro-heme d_1. More importantly, the absorption spectrum of the NirF/dihydro-heme d_1 mixture recorded directly after mixing the protein with the cofactor did not change further upon prolonged incubation, in contrast to what was observed for the NirN/dihydro-heme d_1 mixture (see above). Therefore, we concluded that NirF was able to bind dihydro-heme d_1 but did not convert it to heme d_1.

NirN Catalyzes the Double Bond Formation using Electron Bifurcation—As outlined above, our studies revealed a new and unexpected function of NirN during heme d_1 biosynthesis, namely that of the terminal dehydrogenase introducing the double bond into the propionate side chain of pyrrole ring D of dihydro-heme d_1 to yield the acrylate side chain of heme d_1. However, NirN must be a quite unusual dehydrogenase because it did not require the addition of any cofactor such as NAD^+ or FAD/FMN typically employed by common dehydrogenases catalyzing two-electron oxidation reactions. Interestingly, in our initial NirN/dihydro-heme d_1 reaction described above, we observed that the produced heme d_1 was in the reduced Fe(II) state, although the substrate dihydro-heme d_1 entered the reaction mixture in the oxidized Fe(III) form. Therefore, it seemed that one electron of the two-electron oxidation remained on the reaction product itself. Nevertheless, the fate of the second electron was still unclear. In this context, it is important to note that NirN contains a covalently attached heme *c* cofactor (16), and, therefore, we speculated that the second electron might be transferred to the heme *c*. In the initial reaction mixture, no reduction of the heme *c* in NirN was observed. However, this reaction was performed under aerobic conditions, which might have led to a rapid reoxidation of any reduced heme *c*. Therefore, we repeated the NirN activity assay under anaerobic conditions in an anaerobic chamber. NirN in its oxidized form (*i.e.* containing Fe(III)-heme *c*) was mixed with oxidized Fe(III)-dihydro-heme d_1, and the reaction pro-

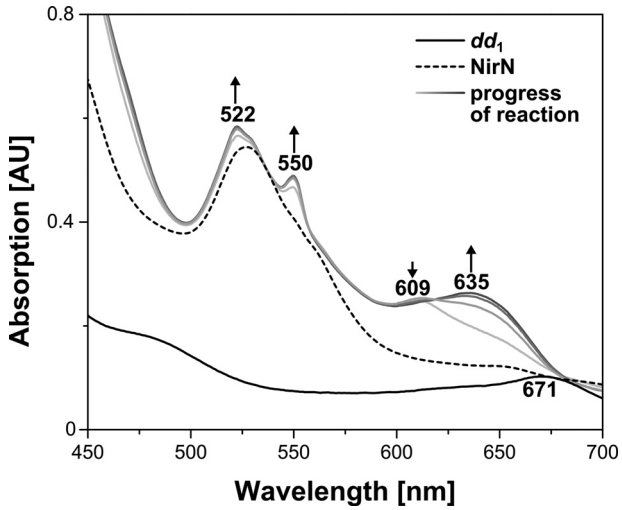

FIGURE 8. **NirN activity assay under anaerobic conditions.** UV-visible absorption spectra of free dihydro-heme d_1 (dd_1), of purified NirN, and of the NirN/dihydro-heme d_1 reaction mixture incubated under anaerobic conditions in an anaerobic chamber. For the NirN/dihydro-heme d_1 reaction mixture, spectra were measured immediately after mixing the two components (*light gray*) and then every 15 s (from *light* to *dark gray*). Characteristic absorption bands are labeled. The increase or decrease of absorption bands during the reaction progress is indicated by *arrows*. *AU*, absorption units.

gress was followed by UV-visible absorption spectroscopy (Fig. 8). As before, a new absorption band at about 635 nm developed during the reaction, which represents the NirN-bound heme d_1 in its reduced Fe(II) form. Moreover, two new absorption peaks at 522 and 550 nm appeared simultaneously with the absorption band at 635 nm. These absorption features are indeed characteristic for the reduced Fe(II)-heme *c* in NirN (16). On the basis of this experiment, we conclude that NirN catalyzes the two-electron oxidation of dihydro-heme d_1 to heme d_1 using an electron bifurcation mechanism during which one electron ends up on the reaction product heme d_1 and the second electron is transferred to the heme *c* cofactor of the enzyme.

Novel Roles of NirN and NirF during Heme d_1 Biosynthesis and Insertion into NirS—On the basis of the experiments described in this study, we would like to assign a novel function to the NirN protein. So far, the role of NirN was unclear because *nirN* deletion strains did not show extreme growth phenotypes and still produced an active form of NirS, which led to the assumption that NirN was apparently not involved in heme d_1 biosynthesis. However, we observed that the deletion of the *nirN* gene in *P. aeruginosa* resulted in the production of a holo NirS with an obviously altered cofactor content (15). In this study, we could show that this form of holo NirS actually carried the heme d_1 precursor dihydro-heme d_1. Further, we showed that NirN is able to catalyze the conversion of dihydro-heme d_1 to heme d_1 *in vitro*. Therefore, we identified NirN as the terminal dehydrogenase catalyzing the last step of heme d_1 biosynthesis. Moreover, we propose that NirN represents a novel and unusual type of a periplasmic dehydrogenase that uses an electron bifurcation mechanism to catalyze a two-electron oxidation reaction carrying only a one-electron accepting redox cofactor (heme *c*). Such a mechanism is possible for NirN because its substrate/product itself is able to accept one electron.

Considering the finding that NirN catalyzes the last step of heme d_1 biosynthesis, the question arises what the function of NirF might be that was assumed previously to play the role now assigned to NirN. In this study, we observed that NirF is able to bind dihydro-heme d_1. Together with the previous observation that NirF from *P. aeruginosa* is a periplasmic, membrane-anchored lipoprotein that interacts with both NirN and NirS (14, 15), one might speculate that NirF could be involved in the uptake of dihydro-heme d_1 into the periplasm from a still unknown membrane transporter and then further transfer the precursor to NirN. NirN then catalyzes the formation of heme d_1, which is finally transferred to NirS, yielding the active holo form of the enzyme. Such a role of NirF in the uptake of the heme d_1 precursor into the periplasm is, of course, speculative at this stage and will require further research.

Acknowledgments—We thank Dr. Linda Thöny-Meyer (EMPA Materials Science and Technology, St. Gallen, Switzerland) for plasmid pEC86 and Dr. Hiroyuki Arai (Department of Biotechnology, University of Tokyo, Japan) for P. aeruginosa PAO1 strain RM361. We also thank Dr. Jürgen Moser (Institute of Microbiology, Technische Universität Braunschweig, Germany) for discussions and Dr. Dieter Jahn (Institute of Microbiology, Technische Universität Braunschweig, Germany) for support.

REFERENCES

1. Zumft, W. G. (1997) Cell biology and molecular basis of denitrification. *Microbiol. Mol. Biol. Rev.* **61,** 533–616
2. Silvestrini, M. C., Galeotti, C. L., Gervais, M., Schininà, E., Barra, D., Bossa, F., and Brunori, M. (1989) Nitrite reductase from *Pseudomonas aeruginosa*: sequence of the gene and the protein. *FEBS Lett.* **254,** 33–38
3. Fülöp, V., Moir, J. W., Ferguson, S. J., and Hajdu, J. (1995) The anatomy of a bifunctional enzyme: structural basis for reduction of oxygen to water and synthesis of nitric oxide by cytochrome cd_1. *Cell* **81,** 369–377
4. Cutruzzolà, F., Rinaldo, S., Centola, F., and Brunori, M. (2003) NO production by *Pseudomonas aeruginosa* cd_1 nitrite reductase. *IUBMB Life* **55,** 617–621
5. Chang, C. K. (1994) Haem d_1 and other haem cofactors from bacteria. *Ciba Found. Symp.* **180,** 228–238, discussion 238–246
6. Chang, C. K., Timkovich, R., and Wu, W. (1986) Evidence that heme d_1 is a 1,3-porphyrindione. *Biochemistry* **25,** 8447–8453
7. Bali, S., Lawrence, A. D., Lobo, S. A., Saraiva, L. M., Golding, B. T., Palmer, D. J., Howard, M. J., Ferguson, S. J., and Warren, M. J. (2011) Molecular hijacking of siroheme for the synthesis of heme and d_1 heme. *Proc. Natl. Acad. Sci. U.S.A.* **108,** 18260–18265
8. de Boer, A. P., Reijnders, W. N., Kuenen, J. G., Stouthamer, A. H., and van Spanning, R. J. (1994) Isolation, sequencing and mutational analysis of a gene cluster involved in nitrite reduction in *Paracoccus denitrificans*. *Antonie Van Leeuwenhoek* **66,** 111–127
9. Kawasaki, S., Arai, H., Kodama, T., and Igarashi, Y. (1997) Gene cluster for dissimilatory nitrite reductase (*nir*) from *Pseudomonas aeruginosa*: sequencing and identification of a locus for heme d_1 biosynthesis. *J. Bacteriol.* **179,** 235–242
10. Palmedo, G., Seither, P., Körner, H., Matthews, J. C., Burkhalter, R. S., Timkovich, R., and Zumft, W. G. (1995) Resolution of the *nirD* locus for heme d_1 synthesis of cytochrome cd_1 (respiratory nitrite reductase) from *Pseudomonas stutzeri*. *Eur. J. Biochem.* **232,** 737–746
11. Storbeck, S., Walther, J., Müller, J., Parmar, V., Schiebel, H. M., Kemken, D., Dülcks, T., Warren, M. J., and Layer, G. (2009) The *Pseudomonas aeruginosa nirE* gene encodes the *S*-adenosyl-L-methionine-dependent uroporphyrinogen III methyltransferase required for heme d_1 biosynthesis. *FEBS J.* **276,** 5973–5982
12. Zajicek, R. S., Bali, S., Arnold, S., Brindley, A. A., Warren, M. J., and Fer-

guson, S. J. (2009) d_1 haem biogenesis: assessing the roles of three *nir* gene products. *FEBS J.* **276,** 6399–6411
13. Bali, S., Warren, M. J., and Ferguson, S. J. (2010) NirF is a periplasmic protein that binds d_1 heme as part of its essential role in d_1 heme biogenesis. *FEBS J.* **277,** 4944–4955
14. Remans, K., Vercammen, K., Bodilis, J., and Cornelis, P. (2010) Genome-wide analysis and literature-based survey of lipoproteins in *Pseudomonas aeruginosa*. *Microbiology* **156,** 2597–2607
15. Nicke, T., Schnitzer, T., Münch, K., Adamczack, J., Haufschildt, K., Buchmeier, S., Kucklick, M., Felgenträger, U., Jänsch, L., Riedel, K., and Layer, G. (2013) Maturation of the cytochrome cd_1 nitrite reductase NirS from *Pseudomonas aeruginosa* requires transient interactions between the three proteins NirS, NirN and NirF. *Biosci. Rep.* 10.1042/BSR20130043
16. Hasegawa, N., Arai, H., and Igarashi, Y. (2001) Two *c*-type cytochromes, NirM and NirC, encoded in the *nir* gene cluster of *Pseudomonas aeruginosa* act as electron donors for nitrite reductase. *Biochem. Biophys. Res. Commun.* **288,** 1223–1230
17. Li, Y., Bali, S., Borg, S., Katzmann, E., Ferguson, S. J., and Schüler, D. (2013) Cytochrome cd_1 nitrite reductase NirS is involved in anaerobic magnetite biomineralization in *Magnetospirillum gryphiswaldense* and requires NirN for proper d_1 heme assembly. *J. Bacteriol.* **195,** 4297–4309
18. Arslan, E., Schulz, H., Zufferey, R., Künzler, P., and Thöny-Meyer, L. (1998) Overproduction of the *Bradyrhizobium japonicum c*-type cytochrome subunits of the cbb_3 oxidase in *Escherichia coli*. *Biochem. Biophys. Res. Commun.* **251,** 744–747
19. Studier, F. W. (2005) Protein production by auto-induction in high density shaking cultures. *Protein Expr. Purif.* **41,** 207–234
20. Tartoff, K. D., and Hobbs, C. A. (1987) Improved media for growing plasmid and cosmid clones. *Bethesda Res. Lab. Focus* **9,** 12
21. Heydorn, A., Nielsen, A. T., Hentzer, M., Sternberg, C., Givskov, M., Ersbøll, B. K., and Molin, S. (2000) Quantification of biofilm structures by the novel computer program COMSTAT. *Microbiology* **146,** 2395–2407
22. Parr, S. R., Barber, D., and Greenwood, C. (1976) A purification procedure for the soluble cytochrome oxidase and some other respiratory proteins from *Pseudomonas aeruginosa*. *Biochem. J.* **157,** 423–430
23. Spiro, T. G. (1985) Resonance Raman spectroscopy as a probe of heme protein structure and dynamics. *Adv. Protein Chem.* **37,** 111–159
24. Parthasarathi, N., Hansen, C., Yamaguchi, S., and Spiro, T. G. (1987) Metalloporphyrin core size resonance Raman marker bands revisited: implications for the interpretation of hemoglobin photoproduct Raman frequencies. *J. Am. Chem. Soc.* **109,** 3865–3871
25. Ching, Y., Ondrias, M. R., Rousseau, D. L., Muhoberac, B. B., and Wharton, D. C. (1982) Resonance Raman spectra of heme *c* and heme d_1 in *Pseudomonas* cytochrome oxidase. *FEBS Lett.* **138,** 239–244
26. Choi, S., Spiro, T. G., Langry, K. M., and Smith, K. M. (1982) Vinyl influences on protoheme resonance Raman spectra: nickel(II) protoporphyrin IX with deuterated vinyl groups. *J. Am. Chem. Soc.* **104,** 4337–4344
27. Choi, S., Spiro, T. G., Langry, K. M., Smith, K. M., Budd, D. L., and La Mar, G. N. (1982) Structural correlations and vinyl influences in resonance Raman spectra of protoheme complexes and proteins. *J. Am. Chem. Soc.* **104,** 4345–4351
28. DeVito, V., and Asher, S. A. (1989) UV resonance Raman enhancement of vinyl stretching in ferric protoporphyrin IX: conjugation and preservation of the vinyl .pi. .fwdarw. .pi.* transition. *J. Am. Chem. Soc.* **111,** 9143–9152
29. Lee, H., Kitagawa, T., Abe, M., Pandey, R. K., Leung, H.-K., and Smith, K. M. (1986) Characterization of low frequency resonance Raman bands of metallo-protoporphyrin IX: observation of isotope shifts and normal coordinate treatments. *J. Mol. Struct.* **146,** 329–347
30. Steup, M. B., and Muhoberac, B. B. (1989) Preparation and spectral characterization of the heme d_1.apomyoglobin complex: an unusual protein environment for the substrate-binding heme of *Pseudomonas* cytochrome oxidase. *J. Inorg. Biochem.* **37,** 233–257
31. Walsh, T. A., Johnson, M. K., Barber, D., Thomson, A. J., and Greenwood, C. (1981) Studies on heme d_1 extracted from *Pseudomonas aeruginosa* nitrite reductase. *J. Inorg. Biochem.* **14,** 15–31
32. Oellerich, S., Wackerbarth, H., and Hildebrandt, P. (2002) Spectroscopic characterization of nonnative conformational states of cytochrome *c*. *J. Phys. Chem. B* **106,** 6566–6580